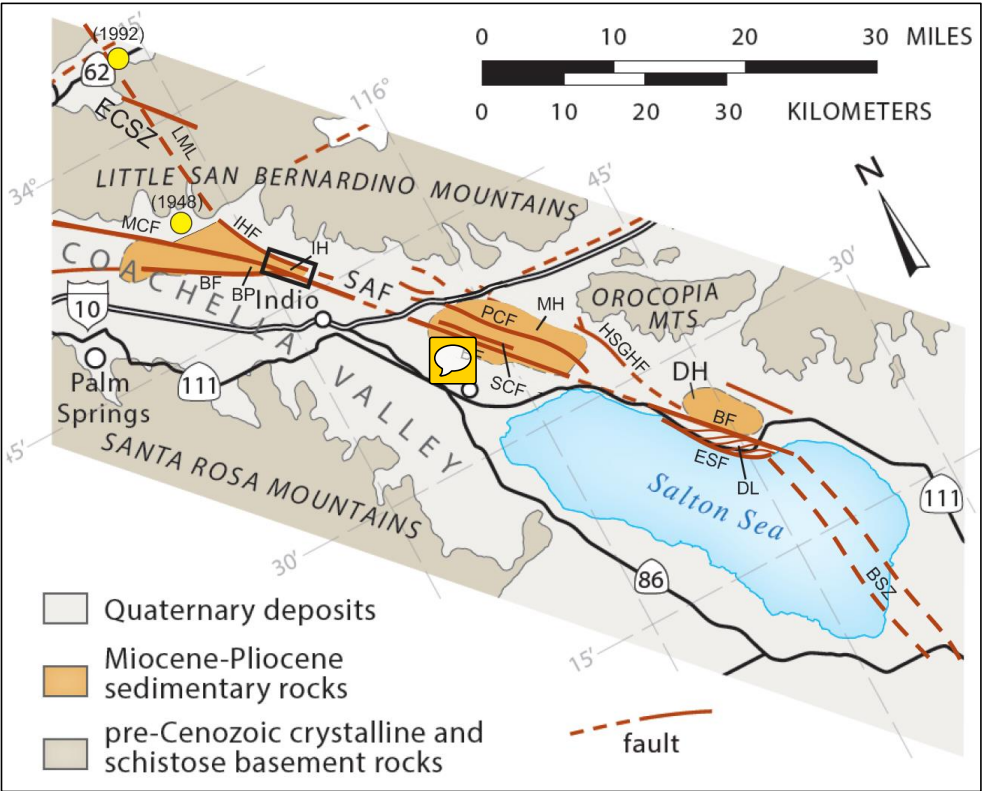
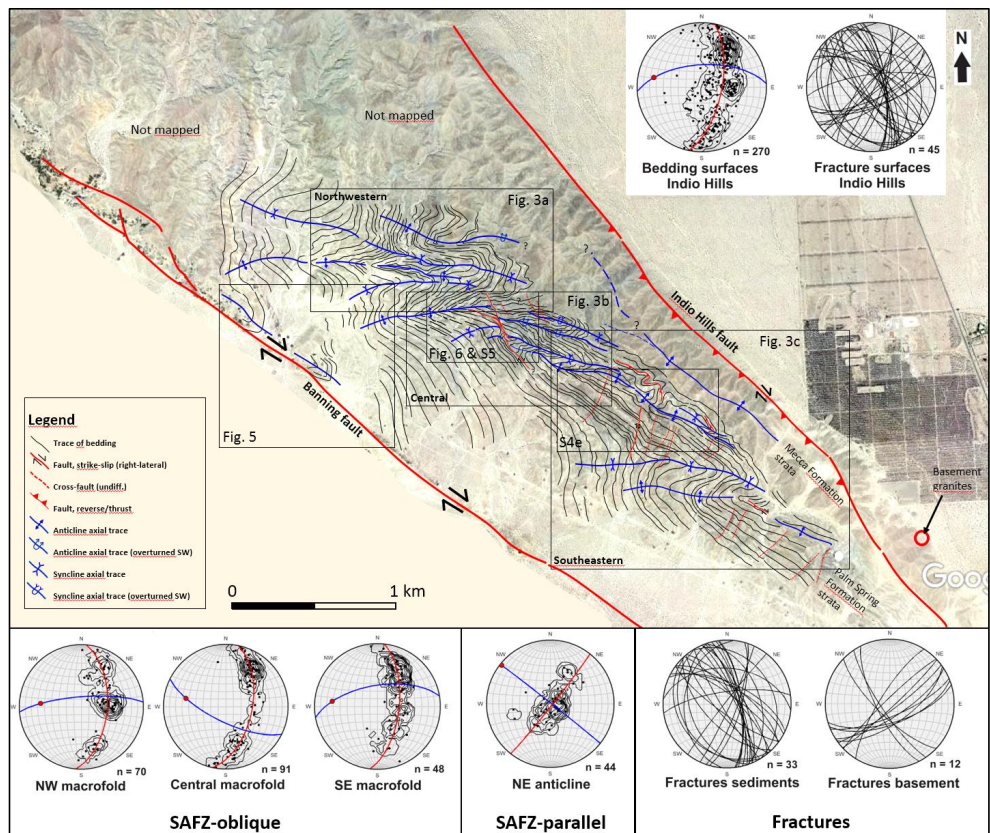




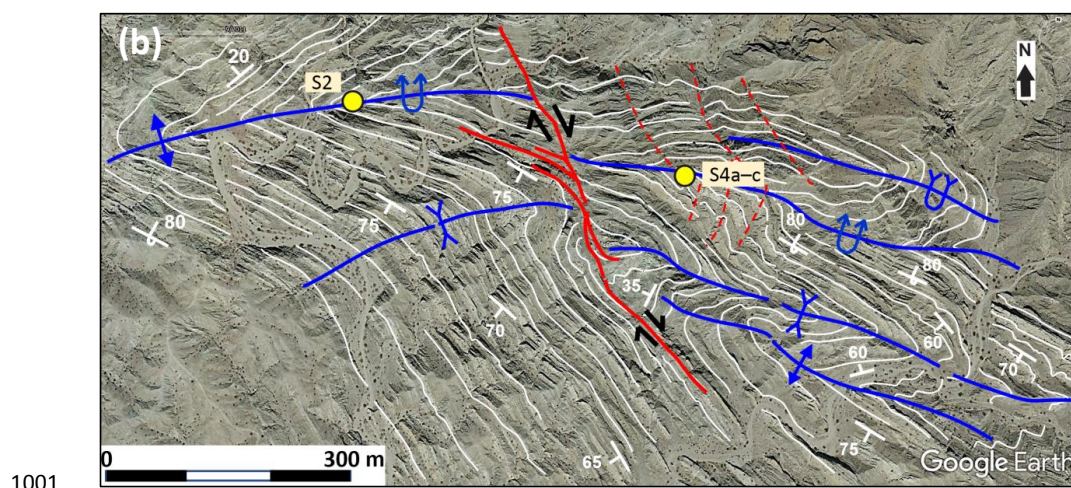
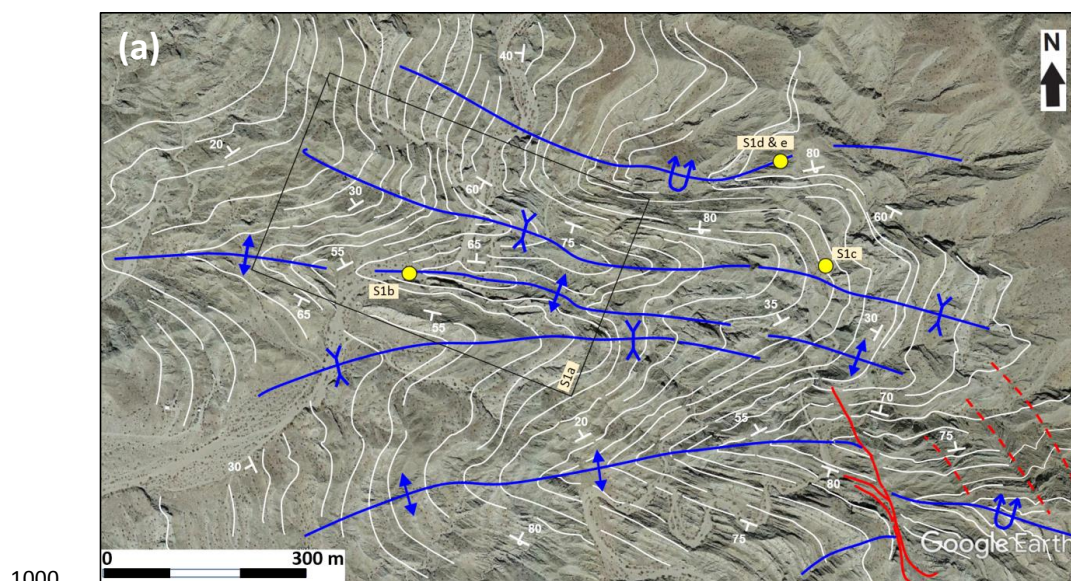
977 **Figures**



978
979 **Figure 1: Simplified geological map of the Coachella Valley and Salton Trough, southern**
980 **California, showing the three main transpressional uplift areas along the SAFZ: the**
981 **Indio Hills (IH), Mecca Hills (MH), and Durmid Hills (DH). Note the link of the SAFZ**
982 **with the Brawley seismic zone to the south. The study area is shown in a black rectangle.**
983 **Recent earthquakes (< 75 years) along the Landers–Mojave Line (LML) are shown as**
984 **yellow dots with associated year of occurrence in parenthesis. Abbreviations: BF:**
985 **Banning Fault; BP: Biskra Palms; DL: Durmid ladder; ECSZ: East California Shear**
986 **Zone; ESF: Eastern Shoreline Fault; HSGHF: Hidden Springs–Grotto Hills fault; IHF:**
987 **Indio Hills fault; LML: Landers–Mojave Line; MCF: Mission Creek Fault; PCF:**
988 **Painted Canyon Fault; SCF: Skeleton Canyon Fault. Modified after Bergh et al. (2019).**



989
990 **Figure 2: Interpreted DEM image in the southeasternmost part of the Indio Hills uplift**
991 **area. Three main SAFZ-oblique macro-folds (northwestern, central, southeastern) are**
992 **mapped in between the bounding Indio Hills and Banning faults, whereas one SAFZ-**
993 **parallel anticline is present close to the Indio Hills fault. More detailed figures are**
994 **numbered and framed. Structural datasets are plotted in lower hemisphere Schmidt**
995 **stereonets. Bedding surfaces are shown as pole to plane with frequency contour lines,**
996 **with average π S great circle (red great circles), fold axial surface (blue great circles) and**
997 **fold axis (red dots). Brittle fractures in sedimentary strata and basement rocks are**
998 **plotted as great circles. Source: Google Earth historical imagery 09-2011. © Google**
999 **Earth 2011.**



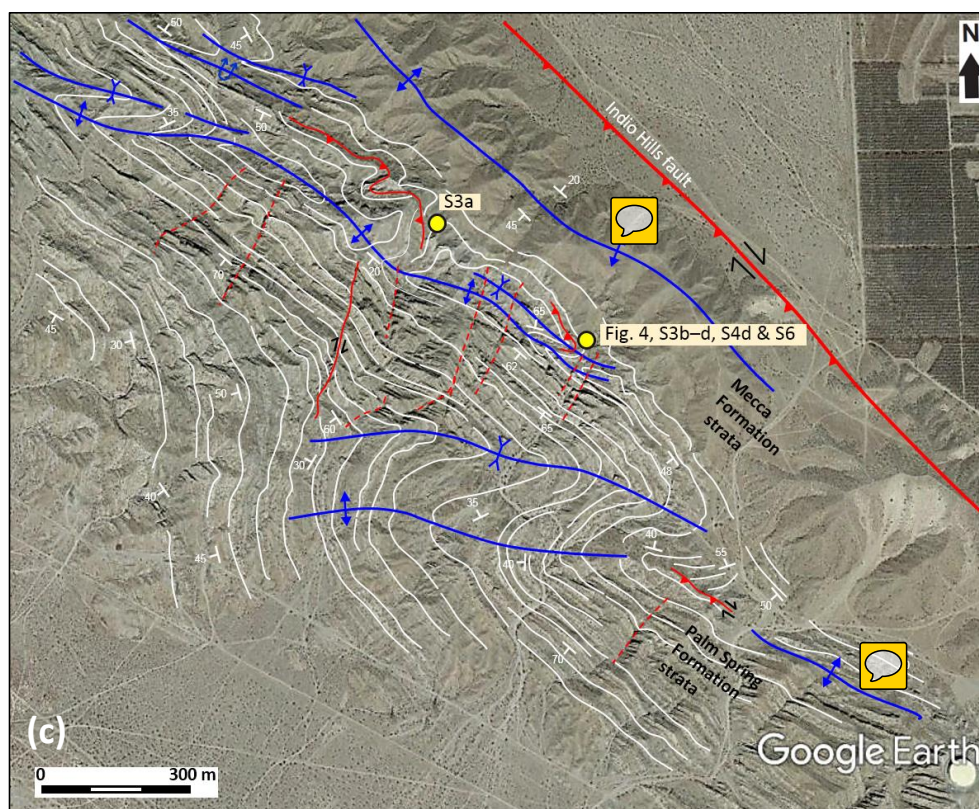


Figure 3: Detailed structural maps showing the architecture and outline of anticline-syncline pairs, traces of bedding and strike and dip orientation, axial surface traces, and fold-related faults in (a) the northwestern, (b) central, and (c) southeastern macro-folds. Note tighter and consistently asymmetric (Z-shaped) geometries of the macro-folds to the east, whereas folds to the west are more open and symmetric. Traces and orientation of bedding show a back-limb composed of attenuated shear folds merging from the central macro-fold in the north, whereas the forelimb is much shorter and more regularly folded. See fig. 2 for legend and location. © Google Earth 2011.

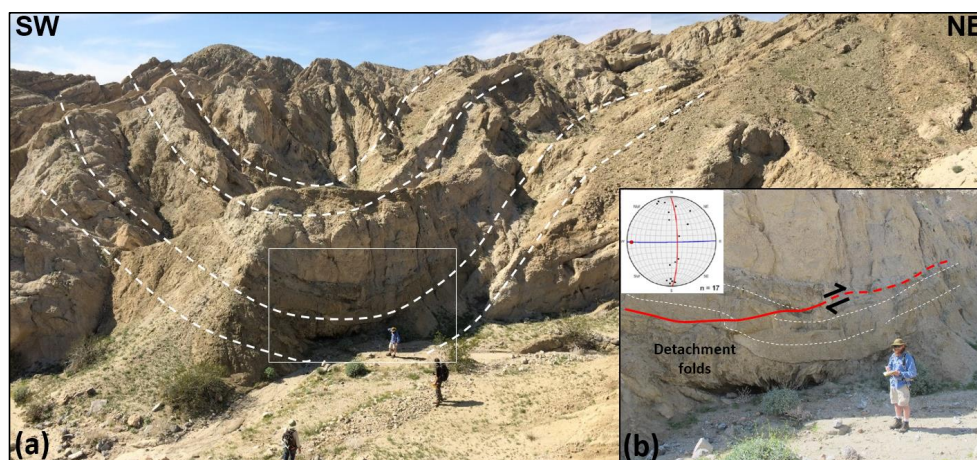


Figure 4: Meso-scale folds and related faults on the back-limb of the southeastern macro-fold. See location in fig. 3c. (a) Syncline in upper Palm Spring Formation units adjacent to the SAFZ-parallel macro-fold near the Indio Hills fault. (b) Close-up view of the synclinal fold hinge in (a), where a meter thick sandstone bed is slightly offset by a minor, low-angle thrust fault (red line) with NE-directed sense-of-shear. The minor thrust faults die out in the overlying sandstone bed. The mudstone bed below acts as a décollement layer with internal, plastically folded lamination, including disharmonic folds. Structural orientation data of minor fold limbs in the décollement zone are plotted in a lower hemisphere Schmidt stereonet, indicating E–W-trending fold axes and a sub-horizontal axial surface (average great circle in red and fold axis as a red dot).

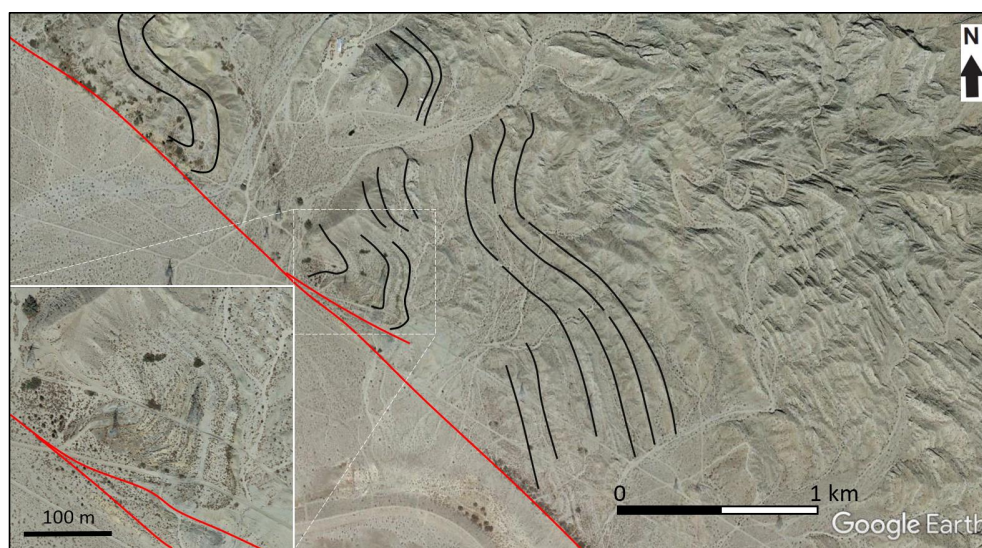


Figure 5: Interpreted SAFZ-parallel macro-folds adjacent to the Banning fault, which affect the southern limb of earlier (*en echelon*) macro-folded and tilted strata of the Palm Spring Formation. Note shear fold geometry in inset map with a thickened hinge zone and thinned limb to the south, and a steeply plunging axis. See fig. 2 for location. © Google Earth 2011.

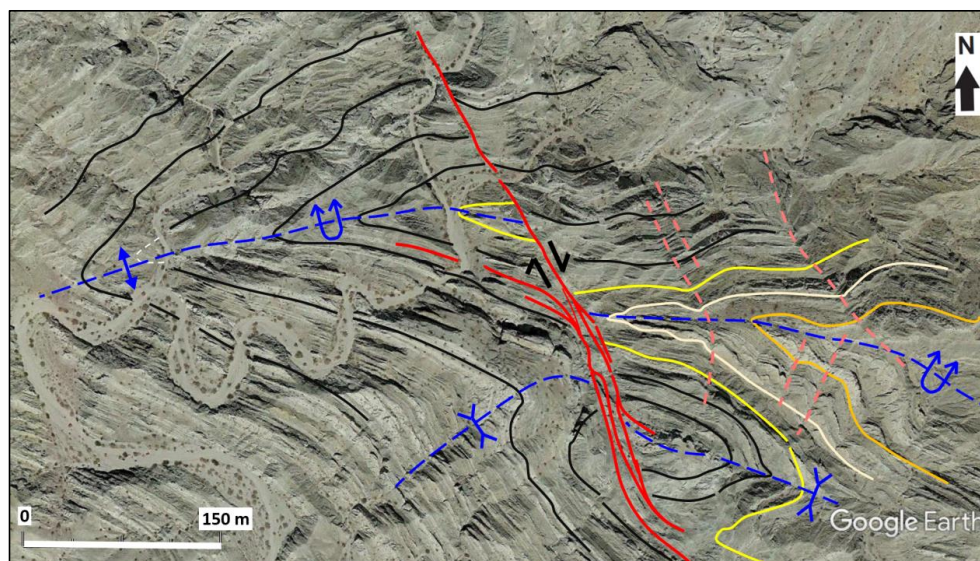


Figure 6: Interpreted satellite image of the central macro-fold showing right-lateral offset of the entire fold hinge/axial surface (upper left dashed blue line) by a NNW–SSE-trending, NE-dipping strike-slip fault (red lines). Note that the fault merges out from a layer in the southern limb of the macro-fold (black lines) and continues as a right-lateral fault. Offset geological markers include thick sandstone beds (yellow, white, light brown lines) and the fold axial surfaces of a second syncline fold farther south (lower right, dashed blue lines). Note that the syncline axial trace dies out to the southwest, and that kink bands acting as cross faults crop out in the eastern part of image (dashed pink lines). Uninterpreted version of the image available as Supplement S5. © Google Earth 2011.

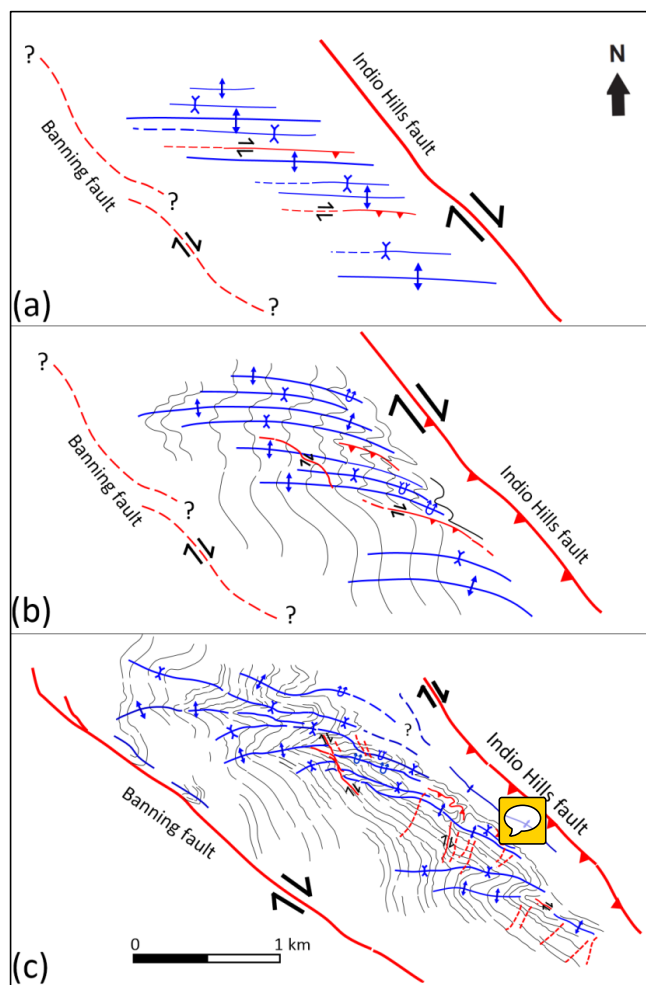
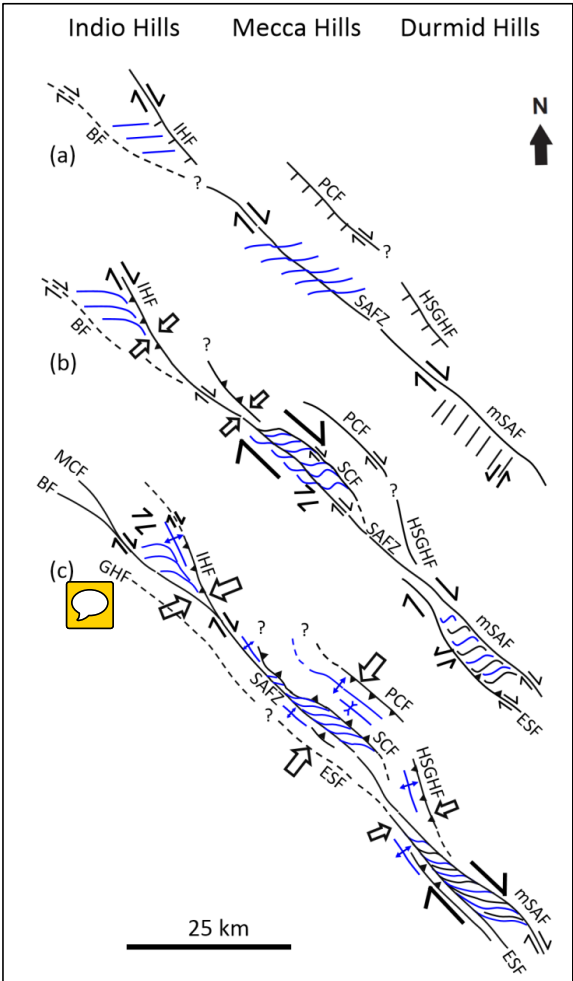


Figure 7: Tentative model illustrating the progressive uplift/inversion history of the Indio Hills presuming a narrow time interval between formation of all structures in the area, except for the Banning fault and associated folds. (a) Early distributed transpressional strain and formation of three major, en-echelon oriented macro-folds, several subsidiary parasitic anticline-syncline fold pairs, and bed-parallel strike-slip and reverse (décollement) faults at a high angle (c. 45°) to the Indio Hills fault. (b) Incremental partly partitioned transpression when the Indio Hills fault started to accommodate oblique-reverse movement forcing previous horizontal *en echelon* macro-folds and parasitic folds to tighten, overturn, and rotate into steeper westward plunges. Note also sigmoidal rotation of axial traces on the back-limbs of the macro-folds to low angle (< 20–30°) with the Indio Hills fault. (c) Late-stage advanced strain partitioning





1051 **with dominant shortening component on the oblique-reverse Indio Hills fault, and right-**
1052 **lateral slip on the Banning Fault. Notice the formation of the anticline parallel to the**
1053 **Indio Hills fault, subsidiary fold-internal strike-slip faults, and conjugate cross faults**
1054 **and kink bands that overprinted the macro-folds. Legend as in fig. 2.**



1055
1056 **Figure 8: Kinematic evolution and along-strike correlation of the Indio Hills, Mecca**
1057 **Hills, and Durmid Hills uplift domains and bounding master faults in the Coachella**
1058 **valley, southern California. We present a progressive kinematic evolution from (a)**
1059 **distributed, through (b) partly partitioned, to (c) advanced partitioned strain events. See**
1060 **text for further explanation. Black lines are faults (full or stippled). Blue lines are fold**
1061 **axial traces. Wide arrows indicate main shortening direction, half-arrows lateral (strike-**
1062 **slip) shearing. Abbreviations: BF: Banning fault; ESF: Eastern Shoreline fault; GHF:**
1063 **Garnet Hills fault; HSGHF: Hidden Springs–Grotto Hills fault; IHF: Indio Hills fault;**
1064 **mSAF: main San Andreas fault in Durmid Hills; MCF: Mission Creek fault; PCF:**
1065 **Painted Canyon fault; SAFZ: San Andreas transform fault; SCF: Skeleton Canyon**
1066 **fault.**